International Journal of Radiation Biology

ISSN: (Print) (Online) Journal homepage: https://www.tandfonline.com/loi/irab20

# Modeling principles of protective thyroid blocking

**Alexis Rump, Stefan Eder, Cornelius Hermann, Andreas Lamkowski, Manabu Kinoshita, Tetsuo Yamamoto, Junya Take, Michael Abend, Nariyoshi Shinomiya & Matthias Port**

**To cite this article:** Alexis Rump, Stefan Eder, Cornelius Hermann, Andreas Lamkowski, Manabu Kinoshita, Tetsuo Yamamoto, Junya Take, Michael Abend, Nariyoshi Shinomiya & Matthias Port (2022) Modeling principles of protective thyroid blocking, International Journal of Radiation Biology, 98:5, 831-842, DOI: 10.1080/09553002.2021.1987570

**To link to this article:** https://doi.org/10.1080/09553002.2021.1987570

© 2021 The Author(s). Published with license by Taylor and Francis Group, LLC

Published online: 11 Nov 2021.

Submit your article to this journal

Article views: 516

View related articles

View Crossmark data

Full Terms & Conditions of access and use can be found at
https://www.tandfonline.com/action/journalInformation?journalCode=irab20

INTERNATIONAL JOURNAL OF RADIATION BIOLOGY
2022, VOL. 98, NO. 5, 831–842
https://doi.org/10.1080/09553002.2021.1987570

Taylor & Francis
Taylor & Francis Group

MINI-REVIEW

OPEN ACCESS Check for updates

# Modeling principles of protective thyroid blocking

Alexis Rump[a], Stefan Eder[a], Cornelius Hermann[a], Andreas Lamkowski[a], Manabu Kinoshita[b], Tetsuo Yamamoto[c], Junya Take[d], Michael Abend[a], Nariyoshi Shinomiya[e], and Matthias Port[a]

[a]Institut für Radiobiologie der Bundeswehr, München, Germany; [b]Department of Immunology and Microbiology, National Defense Medical College, Tokorozawa, Japan; [c]NBC Countermeasure Medical Unit, Japan Ground Self Defense Force, Tokyo Japan; [d]Department of Pediatrics, National Defense Medical College, Tokorozawa, Japan; [e]National Defense Medical College, Tokorozawa, Japan

**ABSTRACT**

**Purpose:** In the case of a nuclear incident, the release of radioiodine must be expected. Radioiodine accumulates in the thyroid and by irradiation enhances the risk of cancer. Large doses of stable (non-radioactive) iodine may inhibit radioiodine accumulation and protect the thyroid ('thyroid blocking'). Protection is based on a competition at the active carrier site in the cellular membrane and an additional temporary inhibition of the organification of iodide (Wolff-Chaikoff effect). Alternatively, other agents like e.g. perchlorate that compete with iodide for the uptake into the thyrocytes may also confer thyroidal protection against radioiodine exposure.

**Purpose:** Biokinetic models for radioiodine mostly describe exchanges between compartments by first order kinetics. This leads to correct predictions only for low (radio)iodide concentrations. These models are not suited to describe the kinetics of iodine if administered at the dosages recommended for thyroid blocking and moreover does not permit to simulate either the protective competition mechanism at the membrane or the Wolff-Chaikoff effect. Models adapted for this purpose must be used. Such models may use a mathematical relation between the serum iodide concentration and a relative uptake suppression or a dependent rate constant determining total thyroidal radioiodine accumulation. Alternatively, the thyroidal uptake rate constant may be modeled as a function of the total iodine content of the gland relative to a saturation amount. Newer models integrate a carrier-mechanism described by Michalis-Menten kinetics in the membrane and in analogy to enzyme kinetics apply the rate law for monomolecular irreversible enzyme reactions with competing substrates to model the competition mechanism. An additional total iodide uptake block, independent on competition but limited in time, is used to simulate the Wolff-Chaikoff effect.

**Conclusion:** The selection of the best model depends on the issue to be studied. Most models cannot quantify the relative contributions of the competition mechanism at the membrane and the Wolff-Chaikoff effect. This makes it impossible or exceedingly difficult to simulate prolonged radioiodine exposure and the effect of repetitive administrations of stable iodine. The newer thyroid blocking models with a separate modeling of competition and Wolff-Chaikoff effect allow better quantitative mechanistic insights and offer the possibility to simulate complex radioiodine exposure scenarios and various protective dosage schemes of stable iodine relatively easily. Moreover, they permit to study the protective effects of other competitors at the membrane carrier site, like e.g. perchlorate, and to draw conclusions on their protective efficacy in comparison to stable iodine.

**ARTICLE HISTORY**
Received 7 July 2021
Revised 20 September 2021
Accepted 22 September 2021

**KEYWORDS**
Medical NRBC-protection; nuclear and radiological emergency; radioiodine; thyroidal protection modeling; iodine blockade; perchlorate

## Objective of thyroid blocking

Nuclear fission processes release a large number of different fission products, including radioactive iodine nuclides. Uranium-235 usually splits asymmetrically and radioiodine(s) fall(s) in one of the favored mass number regions of the fission products (peaks between 90–100 and 130–140). The main radioactive iodine isotopes formed by fission are iodine-131 (physical half-life, $T_{1/2} = 8.02$ d), iodine-129 ($T_{1/2} = 1.57\ 10^7$ y) and iodine-132 ($T_{1/2} = 2.3$ h; from Te-132) (ICRP 2017). Among the different iodine isotopes, iodine-131 is of particular importance (Blum and Eisenbud 1967). Iodine is characterized by its high volatility compared to most other fission products. In the case of nuclear incidents, e.g. nuclear power plant accidents or the detonation of a nuclear weapon, it must be expected that radioiodine will be released and also carried over greater distances (Verger et al. 2001; Chabot 2016). Radioiodine is quickly absorbed into the organism both by inhalation and via ingestion (Geoffroy et al. 2000; Verger et al. 2001). From a practical point of view, intake through contaminated drinking water and food probably plays the decisive role (Blum and Eisenbud 1967).

CONTACT Alexis Rump alexisrump@bundeswehr.org Bundeswehr Institute of Radiobiology Neuherberg Str. 11, Munich D - 80937, Germany

© 2021 The Author(s). Published with license by Taylor and Francis Group, LLC
This is an Open Access article distributed under the terms of the Creative Commons Attribution-NonCommercial-NoDerivatives License (http://creativecommons.org/licenses/by-nc-nd/4.0/), which permits non-commercial re-use, distribution, and reproduction in any medium, provided the original work is properly cited, and is not altered, transformed, or built upon in any way.

After being absorbed into the blood, like natural iodine, radioiodine is quickly absorbed into the thyroid gland where it accumulates. The absorption into the gland takes place via an active transport mechanism (sodium iodide symporter, NI-symporter), which is a saturable process (Eskandari et al. 1997; Darrouzet et al. 2014). The uptake fraction of the total amount of iodine absorbed in the body into the gland shows a high variability from 10 to 40% in healthy euthyroid people (Kovari 1994; Geoffroy et al. 2000; Verger et al. 2001) and may even reach 80% in patients with Grave's hyperthyroidism (Horn-Lodewyk 2019). At the same time as it is absorbed into the gland, iodide is eliminated from plasma unchanged via not saturable renal excretion. The accumulation of radioiodine in the thyroid leads to radiation exposure of the gland, which is associated with an increased risk of the occurrence of tumors (stochastic radiation damages), especially in children and adolescents (Kazakov et al. 1992; Cardis et al. 2005). In addition, radioiodine uptake may result in hypothyroidism, which at lower radiation doses may be the indirect consequence of autoimmune thyroiditis or, at higher radiation doses, the result of cell necrosis or apoptosis (Reiners et al. 2020).

Children are particularly prone to develop thyroid dysfunctions after radioiodine exposure. After the reactor accident in Chernobyl 1986, an enhanced incidence of malignant thyroid tumors was observed in the population exposed to radioiodine as a child (Lomat et al. 1997; Henriksen et al. 2014). After the nuclear weapon test accident on the Marshall Islands in 1954 (Castle Bravo test on the Bikini Atoll), with the inhabitants of the surrounding islands exposed to highly radioactive early local fallout, it was shown that the thyroid gland was a tissue that had absorbed a higher radiation dose from internal compared to external irradiation (Simon et al. 2010). In the following years, an increased incidence of hypothyroidism cases was observed.

The thyroid can be protected against the accumulation of radioiodine by administering a large dose of stable (nonradioactive) iodine shortly before or shortly after radioiodine exposure ('thyroid blocking') (Geoffroy et al. 2000; Verger et al. 2001; Reiners and Schneider 2013; Rump et al. 2016; WHO 2017). This is recommended in case of radioiodine exposure by the World Health Organization (WHO 2017) as well as by many national guidelines (e.g. in France or Germany) (ASN 2008; SSK 2018). The officially recommended dosages may slightly vary (e.g. once 100 mg iodine, i.e. 130 mg potassium iodide in Germany; 76 mg iodine, i.e. 100 mg potassium iodide in Japan) (Yoshida et al. 2014; SSK 2018). For prolonged radioiodine exposure scenarios, as expected in case of power plant accidents as shown in Chernobyl or Fukushima (with much lower releases in the latter case) (Imanaka et al. 2015), there is still a lack of clear cut guidance, although it is acknowledged that repetitive thyroid blocking may be required.

Another pharmacological agent that inhibits the accumulation of iodine in the gland is perchlorate that could be an alternative to stable iodine (Harris et al. 2009; Hänscheid et al. 2011). Quite similarly to iodine, it is rapidly absorbed from the gut with a high systemic bioavailability (95%) and eliminated virtually unchanged by renal excretion with a half-time in the range of 8 h to 12 h (ATSDR 2008; Lorber 2009; BAuA 2016). After the report of several cases of fatal aplastic anemia in the 1960s, its use became very limited in many countries. Meanwhile, there is a resurgence of use in some countries, in particular for the treatment of amiodarone induced thyroid dysfunction, and there are no reports of serious side effects (Wolff 1998; Suwansaksri et al. 2018) that would justify excluding its use for thyroidal protection against iodine-131. However, in official recommendations, it is mostly considered as a second choice agent and moreover perchlorate has no official approval as a medication or is not marketed in all countries (e.g. it is not available anymore in the US or in Japan) (Reference.md 2020). Nevertheless, it seems that it may be advantageous in some scenarios like prolonged radioiodine exposure (Eder et al. 2020).

## Mechanisms of thyroid blocking

Thyroid blocking by large amounts of stable iodine is the result of two mechanisms. As iodide is transported through the basolateral membrane of the thyrocytes by an active saturable transport (NI- symporter), there is a displacement of radioiodide by the excess amount of stable iodide at the carrier site, inhibiting the entry into the cells (Geoffroy et al. 2000; Rump et al. 2019). Meanwhile, the non saturable renal elimination is going on unchanged, rapidly reducing the radioiodide content in plasma.

In addition, there is a second mechanism contributing to thyroidal protection that is known as Wolff-Chaikoff effect and described as a thyroidal uptake block becoming effective when the iodine amount in the gland reaches a saturation level (Geoffroy et al. 2000; Rump et al. 2019, 2021). Actually, this effect is not yet fully elucidated mechanistically. It seems that a reduction of peroxidase activity in the thyrocytes may be involved, resulting in an inhibition of the hormonal synthesis and integration of iodide into thyroglobulin (Wolff 1969; Leung and Braverman 2014). The intracellular concentration of free intracellular iodide would be expected to increase, which is compatible with the view of a 'saturation' effect, and it can be speculated that this might accelerate the amount of iodide flowing back out of the thyrocytes by passive diffusion. Iodide may use the same channels and transporters as chloride that are common to many epithelia and that are also present in the membrane of thyrocytes (Simchowitz 1988; Fong 2011). Thus, the net iodide flow through the basolateral thyrocyte membrane into the gland would come to a standstill, corresponding to a complete net uptake block. This latter effect can be expected to add to the decreased accumulation of radioiodine in the gland. There are indications that the competition at the carrier site is the main protective mechanism (2/3 of protective efficacy) with the Wolff-Chaikoff effect contributing in a second place (1/3) (Rump et al. 2019). However, at the difference from competition for the membrane transport, the Wolff-Chaikoff effect is a temporary effect described to last

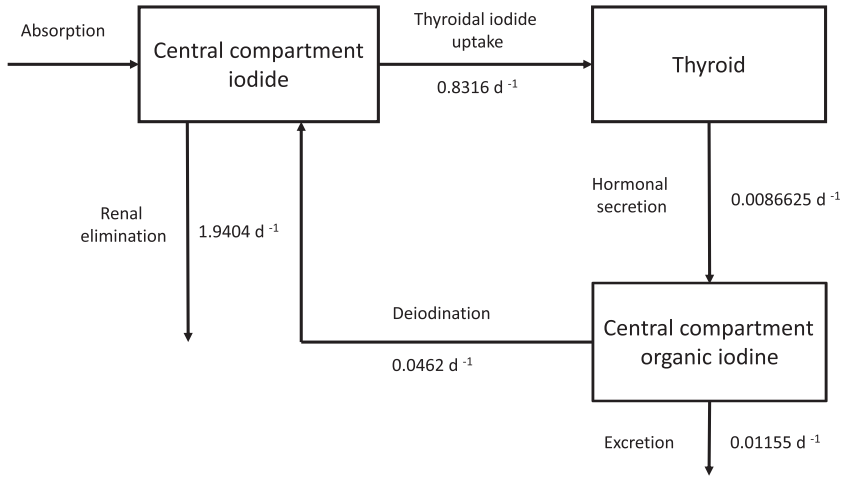


**Figure 1.** Simple three-compartment biokinetic model developed by Riggs (1952) and adopted for many years by the ICRP. For simplification, compartments related to the inhalational absorption or ingestion are omitted. The central compartments contain all the iodide or organic iodine in the body, except the amount in the thyroid. All exchange processes between compartments or describing elimination are first order kinetics. Adapted and modified from ICRP (1997).

about 24 to 48 h (Geoffroy et al. 2000; Verger et al. 2001; Leung and Braverman 2014). This limitation in time must be taken into account, in particular when assessing the protective efficacy of stable iodine in prolonged radioiodine exposure that must not be extrapolated from empirical values gained from short-term exposures.

The NI-symporter in the basolateral thyrocyte membrane is not selective for iodide, but shows affinity for several related monovalent anions, among them perchlorate (Wolff 1964, 1998). Perchlorate has even a higher affinity for the NI-symporter than iodide (Wolff 1998; Eder et al. 2020). Therefore, similarly to stable iodine, perchlorate displace radioiodine from the carrier site and thus reduces radioactivity accumulation in the thyroid gland. However, there are no indications that perchlorate interferes with the organification of iodide after its intracellular uptake as in the case of iodine with the Wolff-Chaikoff effect (Wolff 1998). That's why, despite its higher affinity to the carrier, perchlorate has a lower protective potency (i.e. a higher median effective dose) and to reach a very high protection level as offered by 100 mg stable iodine a larger dose of 1000 mg is required (Hänscheid et al. 2011; Eder et al. 2020). This dosage is however in a range as officially approved in Germany for the initial treatment of hyperthyroidism (Gelbe Liste 2019). From a theoretical point of view, the simple competition mechanism involved in thyroid blocking by perchlorate may be advantageous as the uncertainties associated with the temporary Wolff-Chaikoff effect are avoided (Eder et al. 2020).

## General aspects of biokinetic models for internal dosimetry

In pharmacology and toxicology, kinetic models are used to describe the concentration over time curve of pharmacological or toxic agents in compartments that are accessible for analysis (e.g. blood). The objective is not necessarily to create an image of the anatomical-physiological reality and an assignment of the compartments (usually 1, 2 or 3 compartments) to individual organs or tissues is not clearly possible. In the context of pharmacokinetic-pharmacodynamic (PKPD) modeling, an effect compartment can be added to the kinetic model in order to establish a relation between the concentration of an active agent and the intensity of an acute effect based on a pharmacodynamic model (e.g. for muscle relaxants, opioids etc.) (Sheiner et al. 1979; Lötsch 2005).

In internal dosimetry, physiologically-oriented models, mostly based on a circulatory model, with the clearest possible assignment of the compartments to organs and tissues, must be used. This type of models is also used successfully in toxicology and are of particular importance in case of summation poisons, i.e. when effects are not only dependent on concentrations (like e.g. muscle relaxants, opioids), but on the area under the concentration-time curve (Krishnan and Peyret 2009). When setting up such a model, first, the target organs of the toxic effect are modeled, if necessary by defining several (sub)compartments. In a further step, the uptake and elimination paths are shown, followed by the modeling of further tissues, which should be kept as simple as possible.

Exchange processes between compartments are often based on passive diffusion processes and thus best described by first-order kinetics with a system of differential equations (Derendorf and Garrett 1987). In the case of radionuclides, it must be taken into account that the radioactive exponential decay represents an additional discharge from the compartment that must be mathematically included. The number of radioactive disintegrations (time integrated activity, cumulated activity) in the different compartments is moreover the base to calculate the radiation and energy emitted and at the same time absorbed in the same (e.g. alpha particles with a short range) or also in other compartments (gamma-emitters, use of SAF specific absorbed fractions) (MIRD formalism) (Loevinger et al. 1991; Wessels et al. 2006). The specific absorbed fraction (SAF) is the fraction of emitted energy resulting from radioactive disintegration in a source organ that is absorbed per unit mass of a target organ (Asl et al. 2017). The energy dose permits to

determine the equivalent dose absorbed by the different tissues and organs by multiplication with a factor characterizing the type of radiation and moreover, by applying tissue weights related to the sensitivity for stochastic damages and adding the values for the different tissues, the resulting effective dose absorbed by the body. Physiologically-oriented models are easy to imagine, but on the other hand determining valid parameters (transfer rates between compartments) for humans may be a challenge. Moreover, the mathematical manageability of the model is important, but fortunately special software packages are available for calculations in internal dosimetry (e.g. Integrated Modules for Bioassay Analysis, IMBA) (Birchall et al. 2007).

The International Commission on Radioprotection provides several biokinetic models for internal dosimetry. Generic models were set up for a larger group of elements, such as the model of the respiratory tract (ICRP 1994a), the gastrointestinal tract (ICRP 1979) or the wound model (Guilmette et al. 2007; NCRP 2007). The systemic models that describe the disposition of radionuclides after their transition into the blood, on the other hand, show a stronger differentiation depending on the respective element. By combining the appropriate sub-models (absorption by inhalation and/or ingestion + systemic), it is possible to construct a comprehensive model for the disposition of a radionuclide corresponding to the concrete situation to study.

## Radioiodine biokinetic models

Different physiological models of various complexity have been developed to describe the systemic disposition of iodine (Riggs 1952; ICRP 1994b, 1997; Leggett 2010; ICRP 2017). A simple three-compartment biokinetic model developed by Riggs (1952) was adopted for many years by the ICRP to describe radioiodine intake and disposition in occupational and environmental settings (ICRP 1994b, [ICRP] International Commission on Radiological Protection 1997) (Figure 1). Following absorption, the model describes the uptake of iodide (inorganic iodine) from the 'blood' (central compartment) into the thyroid as well as its renal elimination out of the body. Moreover, the secretion of organic iodine (thyroid hormones) and its further disposition (elimination through feces, deiodination and release into the iodide pool) is represented. As iodine is rapidly and completely absorbed by inhalation or ingestion, it seems legitimate for kinetic simulations to enter radioiodine directly into the central compartment like for an intravenous injection without modeling in addition the absorption process through the lungs or the gastrointestinal tract. It is worth mentioning that the secretion of organic iodine out of the thyroid is a very slow process (0.0086625 $d^{-1}$, $T_{1/2} = 80$ d) compared to thyroidal iodide uptake from the central iodide compartment (rate constant 0.8316 $d^{-1}$, $T_{1/2} = 20$ h). Organic iodine release from the gland is also a relatively slow process in comparison to the physical decay of iodine-131 ($T_{1/2}$ = 8 days). To simplify computations, for practical purposes it seems therefore legitimate to perform dosimetric calculations using the model without taking into account the hormonal secretion out of the gland (Rump et al. 2019; Eder et al. 2020). The error by this omission can be viewed as negligible, all the more since the thyroid clearance shows a very high physiological variability.

Although the three-compartment model described above should be considered as very useful for practical purposes, the disposition of inorganic and organic iodine seems to be actually more complex. This led to the development of models using several interconnected compartments to represent the thyroid permitting to better understand iodine trapping by organification in the gland (Hays 1978). A more elaborate biokinetic model including additional tissue compartments and an exchange with the gastrointestinal tract that was originally developed by Leggett (2010) was meanwhile adopted by the ICRP (2017). For the sake of completeness, it should be mentioned that other models intended for special subpopulations have been developed, e.g. to describe the age-dependent iodine disposition in children (Leggett 2017) or in pregnant or breastfeeding women, including the possibility to assess the dose absorbed by the thyroid of the embryo/fetus depending on the gestational age or the nursing infant (Berkovski 2002).

All the mentioned models use first order kinetics with given invariable rate constants to describe exchange processes between compartments. This is correct when describing a flux driven by diffusion, but only legitimate as an approximation in the case of saturable processes (e.g. carrier mediated transport) when substrate concentrations are very low. A carrier-mediated transport can be described in analogy to enzyme reactions by Michaelis-Menten kinetics (Equation (1)). Only if the concentration of the substrate is very low in comparison to the Michaelis-Menten (affinity) constant $K_m$, the use of first order kinetics may be used as an approximation (Equation 2, rate constant $k = T_{max}/K_m$):

$$T = (T_{max} * C)/(K_m + C) \tag{1}$$

$$\begin{aligned} T &= (T_{max} * C)/(Km + C) \\ &= (T_{max} * C)/Km \\ &= (T_{max}/Km) * C = k * C \end{aligned} \tag{2}$$

T ($\mu mol*l^{-1}*d^{-1}$) is the transport capacity through the membrane at the time when C ($\mu mol*l^{-1}$) is the concentration of iodide in the extracellular space. The Michaelis-Menten constant ($K_m$) ($\mu mol*l^{-1}$) and the maximum transport capacity ($T_{max}$) ($\mu mol*l^{-1}*d^{-1}$) are the parameters of the equation. If C is very small compared to $K_m$, so that the process can be approximated to first order kinetics, the quotient $T_{max}/K_m$ corresponds to the first order rate constant k ($d^{-1}$).

In the case Michaelis-Menten kinetics are used to describe an exchange process between two compartments, it may be convenient to use molar substance amounts instead of concentrations. This requires to know the volume of distribution of the source compartment ($V_s$ in l). In that case C becomes m (= $C*V_s$ in μmol), Km becomes $K_m^{\#}$ (= $K_m*V_s$ in μmol). T and $T_{max}$ are also multiplied by $V_s$ and $T_{max}^{\#}$ expressed in $\mu mol*d^{-1}$. The equation with its original units is probably more familiar to most scientists as Michaelis-Menten kinetics are often associated with enzyme

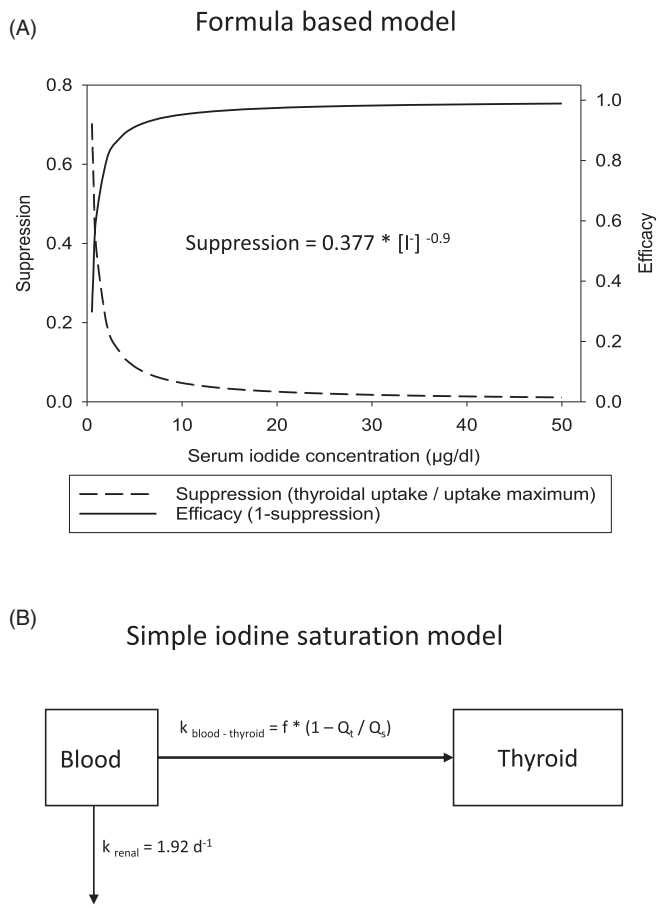


**Figure 2.** (A) Thyroid blocking model based on an empirically-derived relation between the serum iodide concentration and the suppression of radioiodine accumulation in the thyroid (supression = radioiodine uptake/maximum uptake; efficacy = 1 - supression) (Blum et al. 1967). (B) Saturation model expressing the rate constant of iodide transport from blood into the thyroid as a linear function of the total iodine content in the gland relative to a saturation amount (Ramsden et al. 1967). In Figure (B) only the part of the model showing the principle of thyroid blocking has been shown and additional compartments of the original model (e.g. for organic iodine or related to absorption) have been voluntarily omitted for simplification. For saturation values see Table 2.

kinetics, but the derived variable units are probably more convenient when running computations using a compartment model with Michaelis-Menten kinetics describing a saturable transport process.

The Michaelis-Menten (affinity) constant for the NI-symporter transporting iodide has been given with 20–40 µmol*l$^{-1}$ for several species (mouse, rat and sheep thyroids) (Rall et al. 1964) and a lower value of 9 µmol*l$^{-1}$ for humans (Darrouzet et al. 2014). Physiological iodide concentrations in plasma are below 10 µg*l$^{-1}$ (0.08 µmol*l$^{-1}$) (Michalke et al. 1996) and thus very small compared to $K_m$ (9 µmol*l$^{-1}$). Even iodide-131 amounts used in nuclear medicine for the therapy of thyroid diseases (400–3000 MBq, up to several thousand MBq, 8000 MBq) (SSK 1998; Goldsmith 2017) leads to molar concentrations in the extracellular space (assumed distribution volume of iodide in the central compartment 16 l; 8000 MBq, roughly 0.01 µmol/16 l = 6.25*10$^{-4}$ µmol/l) that are far below the $K_m$ of the NI-symporter (Darrouzet et al. 2014). Therefore, the use of first order kinetics to describe carrier-mediated iodide transport processes seems justified in many cases.

The administration of 100 mg iodine however will result in an initial concentration of 49 µmol*l$^{-1}$ in the extracellular space (100 mg/16 l = 788 µmol/16 l) exceeding the $K_m$ value of the carrier. This precludes the use of first order kinetics. Moreover, first order kinetics do not permit to model either competition processes or saturation phenomena (Wolff-Chaikoff effect), at least if the rate constants describing the transport processes are kept constant. Therefore, the described biokinetic models mentioned above are not suited as such to simulate thyroid blocking. They have to be modified for that purpose.

## Approaches to model thyroid blocking

### *A simple formula based model*

Based on a study with volunteers, the relation between the iodide concentration in serum and the inhibition of iodide-131 uptake into the thyroid gland was determined (Blum and Eisenbud 1967). The following non-linear relation between the two variables was fitted (correlation R = 0.96) (Figure 2):

$$\begin{aligned} &\text{Thyroid uptake suppression} \\ &= \text{24-h thyroid uptake/maximum 24-h uptake} \\ &= 0.377 * [I^-]^{-0.9} = 0.0297 * C \end{aligned} \quad (3)$$

with [I$^-$] being the iodide concentration in serum in µg*dl$^{-1}$ and C in µmol*l$^{-1}$.

The mathematical description of the thyroid blockade is not tied to a specific compartment model for iodide and the effects of larger doses of stable iodine on the competition at the carrier site and the Wolff-Chaikoff effect are summarized in the same equation. The relation between the inhibition of iodide uptake into the thyroid gland and the serum iodide concentration, as formulated in the equation, is independent of time and therefore does not take into account that the Wolff-Chaikoff effect is limited in time. Thus, an application of the equation to simulate thyroid blockade is legitimate in the case of acute radioiodine exposure and a single dose of stable iodine for protection, but not in case of prolonged radioiodine exposure and the administration of repeated stable iodine doses. The properties of the model is shown in comparison to other thyroid blocking models in Table 1.

### *A compartmental saturation model*

Whereas in the model of Blum and Eisenbud (1967) the iodide uptake fraction is a function of iodide concentration in serum, thyroid blocking can also be described in a simple three compartment model by expressing the uptake rate constant as a function of the total iodine content of the gland (Ramsden et al. 1967) (Figure 2). This model probably best illustrates the idea of inhibiting iodide uptake by saturating the gland. The rate constant of the transport process from the central compartment into the thyroid is expressed by a linear function:

$$K_{thyr} = f * (1 - Q_t/Q_s) \quad (4)$$

**Table 1.** Comparison of the main properties of the thyroid blocking models.

| | Formula-based model (Blum and Eisenbud 1967) | Saturation model (Ramsden et al. 1967) | Multi-compartment model (Kwon et al. 2020) | Carrier-integrated + WC model (Rump et al. 2019) |
|---|---|---|---|---|
| Separation of modeling of competition and WC-effect | No | No | No | Yes |
| Modeling of prolonged radioiodine exposure and repetitive thyroid blocking | No | difficult | No | Yes |
| Modeling of thyroidal protection by perchlorate | No | No | No | Yes |

WC: Wolff-Chaikoff.

**Table 2.** Differences between biokinetic parameters in models with the same compartment structure for Caucasians (CAU) and Japanese (JPN).

| Parameter | Symbol (unit) | CAU | JPN |
|---|---|---|---|
| Average iodine content of the thyroid | $Q_t$ (mg) | 8.00 | 15 |
| Iodine content of the thyroid at saturation (total uptake block) | $Q_s$ (mg) | 8.35 | 20 |
| Constant related to the transport from the central compartment to the thyroid for an empty gland ($Q_t = 0$) | f ($d^{-1}$) | 23.28 | 1.92 |
| Rate constant of the transport from the central compartment into the thyroid | $K_{thyr}$ ($d^{-1}$) | 0.9758 | 0.4800 |
| Michaelis-Menten (affinity) constant of iodide for the NI-symporter | $K_m$ (μmol) | 9 | 9 |
| Maximum iodide transport capacity from the central compartment into the thyroid | $T_{max}$ (μmol.$d^{-1}$) | 140.52 | 69.12 |

Parameters can be used for simulations with the saturation model of Ramsden et al. (1967) ($k_{thyr}$, f, $Q_t$, $Q_s$) or the model with integrated carrier mechanism and separate Wolff-Chaikoff modeling (Rump et al. 2019, 2021) ($K_m$, $T_{max}$, $Q_t$, $Q_s$). Source of the data: for JPN based on the data of Matsunaga and Kobayashi (2001), for CAU based on the data of Ramsden et al. (1967). Derived values for $T_{max}$ by Rump et al. (2021).

$K_{thyr}$ is the rate constant ($d^{-1}$); $Q_t$ (mg) is the iodine content of the gland; $Q_s$ (mg) is the saturation amount required to completely block iodide uptake into the gland; f ($d^{-1}$) is a notational constant that would correspond to the uptake rate constant in the case of a thyroid fully depleted of iodine ($Q_t$=0 mg). Parameters that have been proposed for this model are given in Table 2 for Caucasians as well as Japanese whose diet differ with a high nutritional daily iodine intake (Ramsden et al. 1967; Matsunaga and Kobayashi 2001; Rump et al. 2021).

The use of a varying rate constant is the expression of non-linear kinetics, even if this does not necessarily have to correspond to Michaelis-Menten kinetics. This is actually not to be expected here, since the inhibition of the uptake of iodide into the thyroid gland is due to two different mechanisms that are mathematically described as a whole in a single simple equation and thus cannot be distinguished. Thus, there is a lack of insight into the quantitative contributions of both mechanisms to the thyroid blockade. Moreover, according to the given equation, the iodide uptake into the gland stops without a time limit when the saturation threshold is reached ($Q_t = Q_s$), and the given equation alone does not allow the time-limited effect of the Wolff-Chaikoff effect to be mapped. Based on results obtained in the volunteer studies, the iodine content of the gland ($Q_t$) could be expressed as a function of the time after administration of stable iodine, which in turn allows conclusions to be drawn about the time course and the recovery of the rate constant that determines iodide uptake into the thyroid ($k_{thyr}$). The model therefore also allows statements to be made about the need for further doses of stable iodine in the event of prolonged exposure to radioiodine. However, the model does not seem suitable for simulating complex exposure scenarios in a simple manner in order to develop optimal stable iodine dosage schemes for thyroid blocking (Table 1).

### *A compartment model with modulation of the intra-thyroidal transfer rate*

Based on the new multicompartment model adopted by the ICRP (Leggett 2010; ICRP 2017) and including two compartments to represent the thyroid with unidirectional transfer, the relation described by Blum and Eisenbud (1967) between the thyroidal iodide uptake fraction and the serum inorganic iodide concentration (Equation 3, see Section V.1) was used to express the intrathyroidal rate constant as a function of the serum iodide concentration (Kwon et al. 2020) (Figure 3):

$$k_{thyr\ 1-2} = k_{thyr\ 1-2\ max} * 0.377 * [I^-]^{-0.9} \quad (5)$$

$[I^-]$ is the iodide concentration in serum (μg*$dl^{-1}$). $k_{thyr\ 1\text{-}2}$ ($d^{-1}$) is the transfer rate from the compartment thyroid 1 to thyroid 2 at a given time point. $k_{thyr\ 1\text{-}2\ max}$ ($d^{-1}$) is the nominal maximum transfer rate at a serum iodide concentration of 0 derived from $k_{thyr\ 1\text{-}2}$ and $[I^-]$ under physiological conditions ($k_{thyr\ 1\text{-}2}$ = 95 $d^{-1}$ and $[I^-]$ = 0.27 μg*$dl^{-1}$) (Kwon et al. 2020).

In this model, non-linear kinetics apply to intrathyroidal iodine transfer that will impact the time course of the iodine content in the thyroidal compartment 1 (iodide), but in particular in the compartment 2 (organic iodine) with a much longer retention time ($k_{thyroid\ 1\ to\ blood\ 1}$ = 36 $d^{-1}$, $T_{1/2}$ = 28 min; $k_{thyroid\ 2\ to\ blood\ 2}$ = 0.0077 $d^{-1}$, $T_{1/2}$ = 90 d; blood 1 contains iodide and blood 2 organic iodine) (Kwon et al. 2020). Thus, the number of radioactive disintegrations will be reduced in compartment 1 and particularly in compartment 2, and the thyroidal equivalent dose diminished accordingly. The uptake of iodide from blood into the thyroidal compartment 1 is not affected by thyroid blocking in the model, suggesting at first sight that the competition mechanism at the carrier site is not taken into account and inhibition occurs solely by reducing the organification

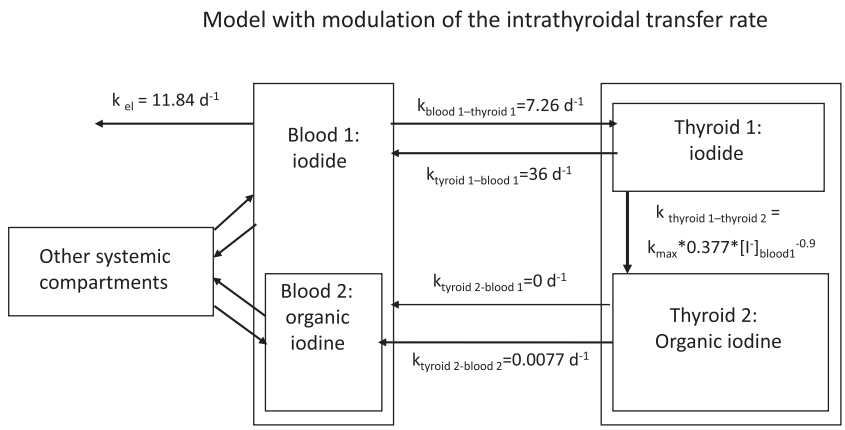


**Figure 3.** Thyroid blocking model based on the modulation of the intra-thyroidal transfer rate from the iodide pool to the organic iodine pool by the serum iodide concentration (Kwon et al. 2020). The model can be viewed as a combination of the multi-compartment model of Leggett (2010) and the empirical equation of Blum and Eisenbud (1967) relating radioiodine uptake suppression to the serum iodide concentration. In the figure, only the part of the model showing the principle of thyroid blocking has been shown and additional compartments of the original model have been voluntarily omitted for simplification.

process. As in the saturation model described in the previous section, both protective mechanisms find their expression in the same equation and in this case the reduced intrathyroidal transfer rate, but again the respective quantitative contributions to thyroidal protection cannot be assessed.

As the intrathyroidal transfer rate is a function of serum iodide concentration, the model seems at first sight quite suited to simulate more complex radioiodine exposure scenarios and different stable iodine dosage schemes as the distribution volume of the central compartment blood 1 can be easily assessed. However, the fixed time-invariable relation between the intrathyroidal transfer rate and the serum iodide concentration may not correctly reflect the Wolff-Chaikoff effect with its limited effectiveness in time (Table 1). This is acknowledged by the authors stating that 'additional adjustments [ … ] beyond reducing the thyroid 1 to thyroid 2 rate are necessary' by considering effects on the transfer from the blood to the thyroid 1 compartment and adjusting the relation with serum iodide concentration (Kwon et al. 2020).

## *A compartment model with integrated NI-symporter and Wolff-Chaikoff effect*

A new approach consists in separating the competition at the carrier from the inhibition of the organification (Wolff-Chaikoff effect) and expressing the thyroid protection as the sum of both effects (Figure 4). The model is derived from the model of Riggs (1952) (Figure 1), and after deleting the compartments for organic iodine, it consists of only two compartments: the central compartment and as second compartment the thyroid acting as a sink. The renal elimination from the central compartment is described by non saturable first order kinetics using the rate constant of the ICRP model of Riggs (see above the section on radioiodine biokinetic models with Figure 1). The transport from the central compartment into the thyroid is modeled by Michaelis-Menten kinetics as for a carrier-mediated transport (see the section on radioiodine biokinetic models and Equation (1)). As the Michaelis-Menten (affinity) constant $K_m$ is a concentration and of major importance for the competition mechanism, the volume of distribution of the central compartment was quantified with 16 l (water: 60% of body weight; extracellular space 1/3, i.e. 14 l and red blood cells about 2 l). For the human NI-symporter, a $K_m$ of 9 µmol*l$^{-1}$ has been reported (Darrouzet et al. 2014) and the maximum transport capacity ($T_{max}$) was derived from the $K_m$ and the constant rate of the ICRP model applicable when the transport process at very low iodide concentrations can be approximated by first order kinetics (see the section on radioiodine biokinetic models and Equation (2) with $k = 0.8316\ d^{-1}$):

$$T_{max} = K_m * k \ = \ 9 * 0.8316 \ = \ 7.48\,\mu mol * l^{-1} * d^{-1}.$$

For modeling the competition at the carrier site, the rate law for monomolecular irreversible enzyme reactions with any number i of competing substrates was used (Chou and Talaly 1977; Schäuble et al. 2013)

$$T1 = \frac{Tmax * C1}{Km1 * \left(1 + \sum_{i=2}^{n} \frac{Ci}{Kmi}\right) + C1} \tag{6}$$

$T_1$ (µmol*l$^{-1}$*d$^{-1}$) is the transport rate for substrate 1; $C_1$ (µmol*l$^{-1}$) the concentration of substrate 1; $K_{ml}$ and $K_{mi}$ (µmol*l$^{-1}$) are he Michaelis-Menten constants for substrate 1 and i respectively, and $T_{max}$ (µmol*l$^{-1}$*d$^{-1}$) the maximum transport rate. In thyroid blocking by stable iodine, the two competing entities are chemically identical (radioiodine and stable iodine) with the same $K_m$. In order to make the calculations easier, all equations were converted so that molar substance amount units (µmol) and not concentrations (µmol*l$^{-1}$) could be entered in the central compartment (Rump et al. 2019). The principle of this conversion has already been mentioned in the section of radioiodine biokinetic models when introducing Michaelis-Menten kinetics. By multiplying the numerator and denominator of the equation describing substrate competition with the distribution volume (extracellular space, volume of the source compartment $V_s$ = 16 l), the concentration C (µmol*l$^{-1}$) becomes a substance amount m (µmol). Similarly, the Michaelis-

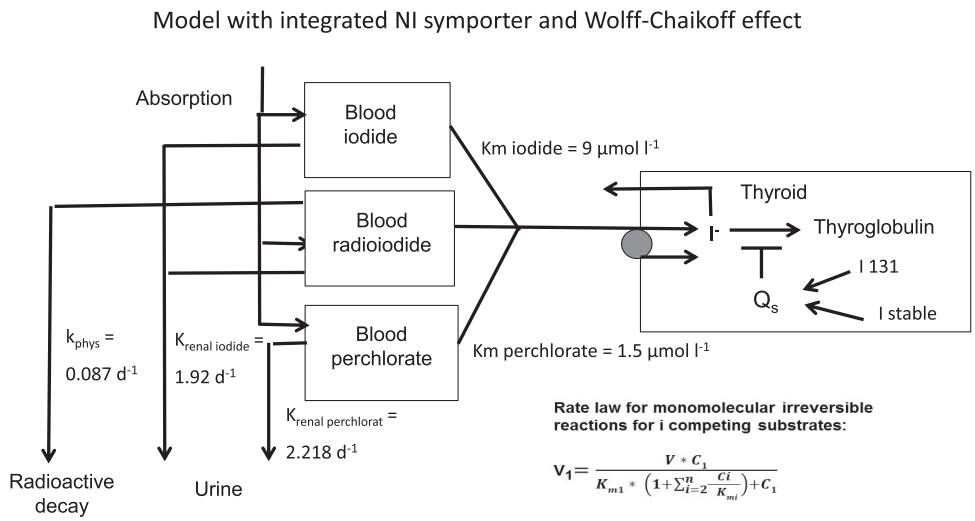


**Figure 4.** Compartment models for radio(iodine) and perchlorate with an integrated carrier uptake mechanism described by Michaelis-Menten kinetics for thyroidal iodide uptake. The competition of radioiodide with stable iodide or perchlorate at the carrier site is modeled by applying the rate law for monomolecular irreversible enzyme reactions to the transport mechanism. The Wolff-Chaikoff effect, only for stable iodide not for perchlorate, is modeled by a total thyroidal uptake block for iodide (lasting 24 h to 48 h), starting when the gland is saturated. Although the models for thyroid blocking by stable iodine and perchlorate are shown on the same figure, protective efficacy of both agents are simulated separately. The physical decay rate constant ($k_{phys} = 0.087\ d^{-1}$) is given for iodine-131 and must be adapted for other radioiodine nuclides.

Menten constant $K_m$ ($\mu mol*l^{-1}$) is also transformed in a substance amount $K_m^{\#}$ ($= K_m*V_s = 9*16 = 144\,\mu mol$). $T_{max}$ is at first derived from $K_m$ and the constant rate k given in the model of Riggs (1952) adopted by the ICRP that is applicable when C is very small compared to $K_m$ and the transport process approaches first order kinetics ($k = 0.8316\ d^{-1}$): $T_{max}=K_m\ *k = 9*0.8316 = 7.4844\,\mu mol*l^{-1}*d^{-1}$ (see the section on radioiodine biokinetic models for the relation between $T_{max}$, $K_m$ and k). In a further step, both sides of the competition equation are multiplied by $V_s$ in order to express the transport capacities for the whole distribution volume per time unit. $T_{max}$ is transformed into $T_{max}^{\#}$ ($=T_{max}*V_s = 7.4844\,\mu mol*l^{-1}*d^{-1} * 16\,l = 119.75\,\mu mol*d^{-1}$). The equations finally used to describe the uptake of radioiodide and stable iodide into the thyroid and their competition are as follows:

$$\text{For radioiodine}: \quad T(I-131) = \frac{119.75\ *m(I-131)}{144 + m\ (I-131) + m\ (I)} \tag{7}$$

$$\text{For stable iodine}: \quad T(I) = \frac{119.75\ *m(I)}{144 + m\ (I-131) + m\ (I)} \tag{8}$$

The model can be easily programmed by using Berkeley Madonna Software and the flow chart function (Macey et al. 2009) that permits to describe transport processes between compartments by first order or more complex kinetics (e.g. Michaelis-Menten kinetics). As compartments are per definition mathematically homogeneous structures, it is necessary to set up the biokinetic model for radioiodide and stable iodide separately and to connect both models in a next step to model the competition mechanism at the carrier site (Figure 5).

The Wolff-Chaikoff effect as the second protective mechanism is modeled by a total thyroidal net uptake block ('switched on' by setting $T_{max}$ at 0, i.e. no transport into the thyroid) becoming effective when the additional iodine content in the gland has reached the saturation level. This has been reported with + 350 µg (2.7581 µmol) (from 8000 µg total iodine content to 8350 µg) (Ramsden et al. 1967). We previously determined this amount with + 448 µg using the data from Blum and Eisenbud (1967), but much higher values have been reported for Japanese (+5000 µg, from 15,000 µg to saturation at 20,000 µg) (Matsunaga and Kobayashi 2001). During the time of total thyroidal uptake block, the renal excretion of iodide is going on unaffected. The thyroidal uptake block is terminated ('switched off') after a defined period of time that is reasonably set between 24–48 h after onset. Different duration can be used for sensitivity analyses.

The weak point of the model is the discrete 'switching on' and 'switching off' of the Wolff-Chaikoff effect, which in reality is certainly a continuous process. The saturation values of the gland and the duration of the effect are also subject to numerous uncertainties, even if the values predicted by the model are well compatible with empirical measurement results on volunteers.

In contrast to the previous approaches, this model allows to quantitatively separate the contributions of the competition at the carrier site and the Wolff-Chaikoff effect, and thus permits to gain mechanistic insights, also for different populations and exposure scenarios (Table 1). It could for example be shown that due to the high average daily nutritional iodine intake by Japanese, the down-regulated maximum transport capacity through the thyrocyte membrane leads on the one hand to a 'natural', albeit inadequate protection against radioiodine exposure, but on the other hand, compared to Caucasians with a lower daily iodine intake, the onset of the Wolff-Chaikoff effect by large doses of stable iodine is delayed (Rump et al.

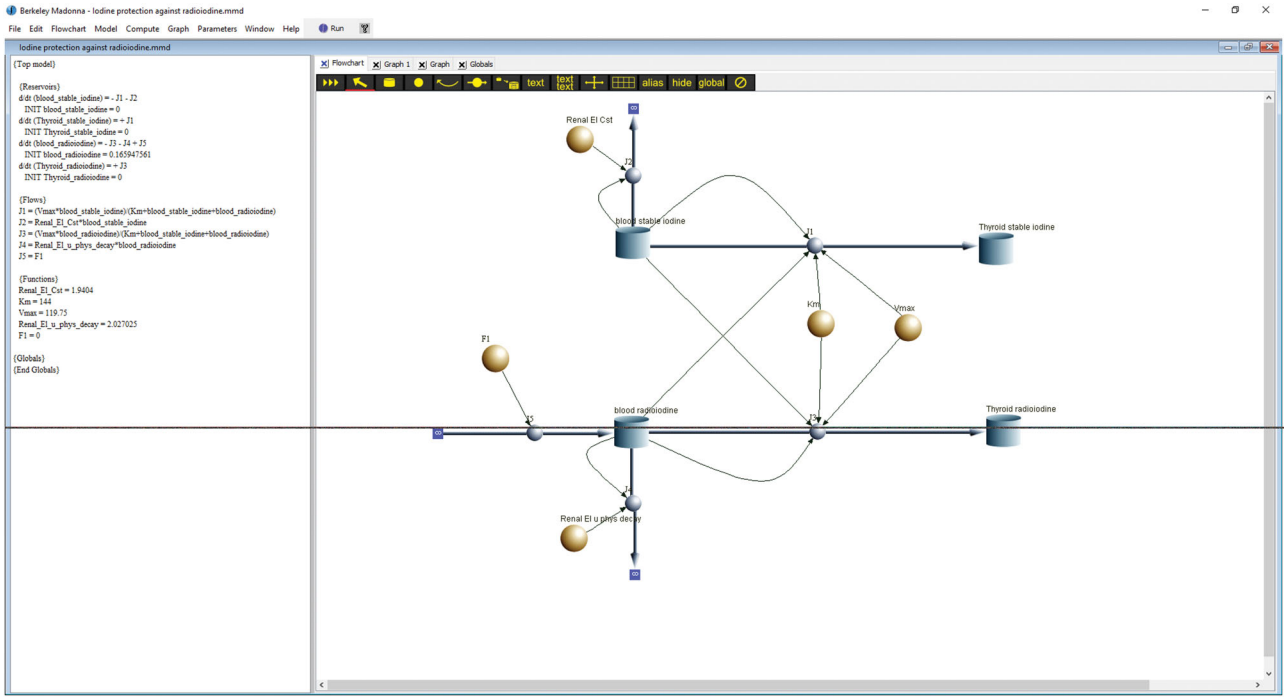


**Figure 5.** Flow chart and equation systems representing thyroid blocking by stable iodine as shown in Figure 4 (Rump et al. 2019, 2021) modeled with Berkeley Madonna software. The complete biokinetic model consists of two separate models for radioiodide and stable iodide that are connected and interact by applying the rate law for monomolecular irreversible enzyme reactions to the transport mechanism. For modeling thyroid blocking by perchlorate (Eder et al. 2020), the model describing stable iodide disposition is replaced by the corresponding perchlorate model differing by the renal elimination rate constant and the Michaelis-Menten constant for the NI-symporter.

2021). In the case of acute radioiodine exposure, this is associated with a lower relative efficacy of the iodine blockade and an almost negligible contribution from the Wolff-Chaikoff effect. However, in the case of prolonged radioiodine exposure, the down-regulated maximum iodide transport capacity has a beneficial effect, even if the differences between Japanese and Caucasians do not seem clinically relevant. A great advantage of the model is the possibility of examining very different exposure scenarios, since the separate inhibition of radioiodine uptake into the gland via competition and the Wolff-Chaikoff effect, with clearly defined time limits for the latter, is not associated with limitations of application or additional computations.

A further unique advantage of the separate treatment of competition and Wolff-Chaikoff effect is the possibility of examining thyroid blocking by agents other than stable iodine (Table 1). This is not possible with all of the models described above with blocking effects by stable iodine summed up in a single equation. As an example, thyroid blockade by perchlorate can be mentioned, with the protection coming about exclusively through competition at the carrier site without effects on the organification process. Applying the model using the $K_m$ values given in the literature for perchlorate shows that in case of acute radioiodine exposure 1000 mg perchlorate achieves the same protective efficacy as 100 mg stable iodine, as described in empirical studies. In case of prolonged radioiodine exposure requiring repetitive daily doses of protective agents, it could be shown that perchlorate seems however to be more advantageous than stable iodine (Eder et al. 2020).

## General aspects of dosimetric computations in thyroid blocking models

A defined radioiodine uptake fraction into the thyroid is required for the use of dose coefficients for inhalation or ingestion to calculate radiological doses. As thyroid blocking is associated with decreased uptake fractions, these dose coefficients may not be used. An easy way to compute thyroid equivalent doses is given by the method of Marinelli/Quimby (Marinelli et al. 1948) for the contribution of the ß-radiation and the geometrical factor method of Hine and Brownell (1956) for the (low) contribution of the ɤ-radiation. The method has also been described for thyroid equivalent dose computations in the more recent literature (National Cancer Institute 2015; Spetz 2010). The dose is given by the following formula:

$$D = C_{max} * T_{eff} * \left(73.8 * \bar{E}ß + 0.0346 * T * \bar{g}\right) \quad (9)$$

D is the total dose from ß and ɤ-radiation (rad), $C_{max}$ the maximum concentration of the radionuclide in tissue ($\mu Ci*g^{-1}$), $T_{eff}$ the effective half-life in the tissue (days) (7.3 days for I-131 in adults), $\bar{E}ß$ the average beta energy (MeV per disintegration) (0.18 MeV for I-131), T the specific ɤ-ray constant ($2.2\,R*mCi^{-1}*h^{-1}$ at 1 cm) and $\bar{g}$ the average geometrical factor for the tissue or organ, equal to 3 $\pi$ r for spheres with radii <10 cm (r = 1.27 cm in adults assuming that the thyroid is made of two identical spheres of unit density) (values from National Cancer Institute 2015). If modeling is done using radioiodine amounts instead of concentrations, the maximum concentration $C_{max}$ is replaced by the maximum accumulated amount divided by the thyroid weight. Although there

are large geographic variations depending on the nutritional iodine supply, an average weight of 17 g seems to be a reasonable estimate (National Cancer Institute 2015; Rump et al. 2021). A transformed but equivalent equation to compute the thyroid equivalent dose is as follow:

$$D\ (\mathrm{mSv}) = 1.647 * 10^{-3} * \text{accumulated I} - 131 \text{ in the thyroid (Bq)} \quad (10)$$

In the case the thyroid is not modeled as a compartment being a perfect sink, but includes an outflow of iodide or organic iodine out of the gland (e.g. in the model with modulation of the intra-thyroidal transfer rate, Kwon et al. 2020), a solution consists in adding an additional compartment to the thyroid (that is not part of the original biokinetic model, with unidirectional outflow from the gland with the physical decay rate constant of iodine-131 $k_{phys}$=0.0866, $T_{1/2}$ = 8.023 d). In this compartment the decayed radioiodine is cumulatively collected expressed in molar amounts like in the biokinetic model. The total number of entities that were decayed can be easily calculated using the Avogadro constant ($6.022*10^{23}\,mol^{-1}$). Applying the mean energy of the emitted ß-radiation (0.18 MeV/decay), it is possible to compute the total energy due to ß-radiation that is absorbed by the gland, and through division by the weight of the thyroid, to get the energy dose (mGy) that is numerically identical to the equivalent dose (mSv), as the factor for ß-radiation is unity. Based on the term under brackets in the extended Quimby/Marinelli equation given above, the relative contribution of the ɤ-radiation can be calculated and added to the dose due to the ß-radiation (ɤ-ray contribution to the total dose about 6% in adults) (Marinelli et al. 1948).

## Conclusion: selecting the right model

The prerequisite for a valid model of thyroidal protection is that the predicted values agree with experimentally measured values in humans. Equivalently, a new model can also be validated by comparing the predicted results with those of an already established model. However, it must be taken into account that experimentally determined data on thyroidal protection in humans are based on simple study designs with the administration of one or a few radioiodine doses for ethical and practical reasons.

The choice of a model depends on the underlying issue. The model should allow answering the question with the greatest possible precision, but in the shortest possible time and with the least possible effort. In our view, simple models should therefore be preferred as far as possible. Models with a large number of compartments may give the impression of greater precision, but compartments that are not really needed also increase the number of parameters required for mathematical description. In addition to the problem of the validity of the parametrization, complex compartment models with a large number of differential equations may lead to the necessity to use particular integration methods to compute the quantities in the compartments from the flows.

Important issues related to thyroidal protection are the choice of the best protective agent with its optimal dosage regimen, especially in the case of complex and prolonged exposure to radioiodine. The great advantage of separating the two mechanisms that contribute to thyroidal protection in the model (carrier competition and Wolff-Chaikoff effect) is that the temporal limitation of the Wolff-Chaikoff effect can easily be taken into account. In particular, this allows very complex radioiodine exposure scenarios and different dosage schemes of stable iodine or other active substances competing with radioiodide at the NI-Symporter to be investigated. Especially with regard to prolonged radioiodine exposure, which are to be expected in the event of power plant accidents with radioiodine release, there is a lack of empirical human data, so that simulation results can be very helpful for planning purposes.

## Ethics approval

Not applicable. This article does not contain any studies with human or animal subjects.

## Consent to participate

Not applicable. This article does not contain any studies with humans.

## Consent for publication

All authors have approved the publication of this study.

## Author contributions

All authors have contributed to the study.

## Disclosure statement

The authors declare that they have no conflicts of interest.

## Funding

The author(s) reported there is no funding associated with the work featured in this article.

## Notes on contributors

*Alexis Rump*, MD, PhD, MHBA, is anesthesiologist and clinical pharmacologist and currently assigned at the Institute of Radiobiology of the Bundeswehr in Munich.

*Stephan Eder*, MD, and Andreas Lamkowski, MD, are physicians, specialists in occupational medicine and researchers in the field of radiobiology.

*Cornelius Hermann* is pharmacist and researcher in radiobiology.

*Andreas Lamkowski* is a physician, specialist in occupational medicine and a researcher at the Bundeswehr Institute for radiobiology.

*Manabu Kinoshita*, MD, PhD is professor at the National Defense Medical College in Tokorozawa (Japan) and specialist in the field of radiobiology.

*Testsuo Yamamoto*, MD, PhD, is the commanding officer of the NBC Countermeasure Medical Unit of the Japan Ground Self Defense Forces.

*Junya Take*, MD, is specialist in pediatrics at the National Defense Medical College Hospital and a researcher in the field of radiobiology.

*Michael Abend*, MD, PhD, MSc, is professor in radiobiology and the deputy director of the Bundeswehr Institute of Radiobiology.

*Nariyoshi Shinomiya*, MD, PhD is professor and the president of the National Defense Medical College.

*Matthias Port*, MD, PhD is professor of internal medicine (hematology/oncology) and radiobiology and the director of the Bundeswehr Institute of Radiobiology.

## ORCID

Alexis Rump http://orcid.org/0000-0002-0492-496X
Manabu Kinoshita http://orcid.org/0000-0002-2750-3084

## Data availability statement

Not applicable. This paper is based on published literature given in the text.

## References

[ATSDR] Agency for Toxic Substances and Disease Registry 2008. Toxicological profile for perchlorates. Atlanta: US Department of Health and Human Services, Public Health Service.

Asl RG, Parach AA, Nasseri S, Momennezhad M, Zakavi SR, Sadoughi HR. 2017. Specific absorbed fractions of internal photon and electron emitters in a human voxel-based phantom: A Monte Carlo study. World J Nucl Med. 16(2):114–121.

[ASN] Autorité de Sureté Nucléaire 2008. Guide national. Intervention médicale en cas d'évènement nucléaire ou radiologique. Version V 3.6. Paris: Autorité de Sureté Nucléaire; [accessed 2021 May 25]. https://www.asn.fr/Professionnels/Les-Guides-de-l-ASN/Guide-national-d-intervention-medicale-en-cas-d-evenement-nucleaire-ou-radiologique.

Berkovski V. 2002. New iodine models family for simulation of short-term biokinetics processes, pregnancy and lactation. Food Nutr Bull. 23(3_suppl1):87–94.

Birchall A, Puncher M, Marsh JW, Davis K, Bailey MR, Jarvis NS, Peach AD, Dorrian MD, James AC. 2007. IMBA Professional Plus: a flexible approach to internal dosimetry. Radiat Prot Dosimetry. 125(1-4):194–197.

Blum M, Eisenbud M. 1967. Reduction of thyroid irradiation from 131 I by potassium iodide. JAMA. 200(12):1036–1116.

[BAuA] Bundesanstalt für Arbeitsschutz und Arbeitsmedizin (Federal Institute for Occupational Safety and Health) 2016. Substance evaluation conclusion as required by REACH 48 and evaluation report for sodium perchlorate. EC No 231-511-9. Dortmund: Bundesanstalt für Arbeitsschutz.

Cardis E, Kesminiene A, Ivanov V, Malakhova I, Shibata Y, Khrouch V, Drozdovitch V, Maceika E, Zvonova I, Vlassov O, et al. 2005. Risk of thyroid cancer after exposure to 131I in childhood. J Natl Cancer Inst. 97(10):724–732.

Chabot G. 2016. Radiation basics. Fission, Fusion. Q10097 - Which fission products are present in a nuclear reactor? Various sources say "many" or hundreds and then refer to 131I, 137Cs, and 90Sr as important products in the case of exposure. Health Physics Society; [accessed 2021 May 25]. https://hps.org/publicinformation/ate/q10097.html#.

Chou TC, Talaly P. 1977. A simple generalized equation for the analysis of multiple inhibitions of Michaelis–Menten kinetic systems. J Biol Chem. 252(18):6438–6442.

Darrouzet E, Lindenthal S, Marcellin D, Pellequer JL, Pourcher T. 2014. The sodium/iodide symporter: State of the art of its molecular characterization. Biochim Biophys Acta. 1838(1 Pt B):244–253.

Derendorf H, Garrett ER. 1987. Pharmakokinetik. Einführung in die Theorie und Relevanz für die Arzneimitteltherapie. Stuttgart: Wissenschaftliche Verlagsgesellschaft.

Eder S, Hermann C, Lamkowski A, Kinoshita M, Yamamoto T, Abend M, Shinomiya N, Port M, Rump A. 2020. A comparison of thyroidal protection by stable iodine or perchlorate in the case of acute or prolonged radioiodine exposure. Arch Toxicol. 94(9):3231–3247.

Eskandari S, Loo DD, Dai G, Levy O, Wright EM, Carrasco N. 1997. Thyroid Na+/I- symporter. Mechanism, stoichiometry, and specificity. J Biol Chem. 272(43):27230–27238.

Fong P. 2011. Thyroid iodide efflux: a team effort? J Physiol. 589(Pt 24):5929–5939.

Gelbe Liste 2019. Fachinformation: Irenat Tropfen 300 mg/ml. Neu Isenburg: Medizinische Medien Informationsdienst GmbH.

Geoffroy B, Verger P, Le Guen B. 2000. Pharmacocinétique de l'iode: revue des connaissances utiles en radioprotection accidentelle. Radioprotection. 35(2):151–174.

Goldsmith SJ. 2017. Radioactive iodine therapy of differentiated thyroid carcinoma: redesigning the Paradigm. Mol Imaging Radionucl Ther. 26(Suppl 1):74–79.

Guilmette RA, Durbin PW, Toohey RE, Bertelli L. 2007. The NCRP wound model: development and application. Radiat Prot Dosimetry. 127(1-4):103–107.

Hänscheid H, Reiners C, Goulko G, Luster M, Schneider-Ludorff M, Buck AK, Lassmann M. 2011. Facing the nuclear threat: thyroid blocking revisited. J Clin Endocrinol Metab. 96(11):3511–3516.

Harris CA, Fisher JW, Rollor EA, Ferguson DC, Blount BC, Valentin-Blasini L, Taylor MA, Dallas CE. 2009. Evaluation of potassium iodide (KI) and ammonium perchlorate (NH4ClO4) to ameliorate 131I- exposure in the rat. J Toxicol Environm Health. 72(14): 897–902.

Hays MT. 1978. Kinetics of the human thyroid trap: a compartmental model. J Nucl Med. 19:789–795.

Henriksen T, Hole EO, Sagstuen E, Pettersen E, Malinen E, Edin NJ, (Biophysics Group at UiO) 2014. Radiation and health. Oslo: University of Oslo, Faculty of mathematics and natural sciences, Department of Physics.

Hine G, Brownell G. 1956. Radiation dosimetry. New York: Academic Press.

Horn-Lodewyk J. 2019. Correlation of radioiodine doses for 6-hr and 24-hour iodine-131 thyroid uptake values for Graves' hyperthyroidism . Endocr J. 66(12):1047–1052.

Imanaka T, Hayashi G, Endo S. 2015. Comparison of the accident process, radioactivity release and ground contamination between Chernobyl and Fukushima-1. J Radiat Res. 56(suppl 1):i56–i61.

[ICRP] International Commission on Radiological Protection1979. Dosimetric model for the gastrointestinal tract. In: ICRP Publication 30 (Part 1). Limits for intakes of radionuclides by workers. Oxford: Pergamon Press. Ann ICRP. 2 (3-4):30-34.

[ICRP] International Commission on Radiological Protection 1994a. Human Respiratory Tract Model for Radiological Protection. ICRP Publication 66. Oxford: Pergamon Press. Ann ICRP. 24(1-3).

[ICRP] International Commission on Radiological Protection 1994b. Dose coefficients for intakes of radionuclides by workers. ICRP Publication 68. Oxford: Pergamon Press. Ann ICRP. 24(4).

[ICRP] International Commission on Radiological Protection 1997. Individual monitoring for internal exposure of workers. Replacement of ICRP Publication 54. ICRP Publication 78. Oxford: Pergamon Press. Ann ICRP. 27(3/4).

[ICRP] International Commission on Radiological Protection 2017. Occupational intakes of radionuclides(Part 3). ICRP Publication 137. Oxford: Pergamon Press. Ann ICRP. 46(3/4).

Kazakov VS, Demidchik EP, Astakhova LN. 1992. Thyroid cancer after Chernobyl. Nature. 359(6390):21.

Kovari M. 1994. Effect of delay time on effectiveness of stable iodine prophylaxis after intake of radioiodine. J Radiol Prot. 14(2):131–136.

Krishnan K, Peyret T. 2009. Physiologically based toxicokinetic (PBTK) modeling in ecotoxicology. In: Devillers J, editor. Ecotoxicology modeling. Dordrecht Heidelberg London New York: Springer; p. 145–176.

Kwon TE, Chung Y, Ha WH, Jin YW. 2020. Application of the new ICRP iodine biokinetic model for internal dosimetry in case of thyroid blocking. Nucl Eng Technol. 52(8):1826–1833.

Leggett R. 2017. An age-specific biokinetic model for iodine. J Radiol Prot. 37(4):864–882.

Leggett RW. 2010. A physiological systems model for iodine for use in radiation protection. Radiat Res. 174(4):496–516.

Leung AM, Braverman LE. 2014. Consequences of excess iodine. Nat Rev Endocrinol. 10(3):136–142.

Loevinger R, Budinger TF, Watson EE. 1991. MIRD primer for absorbed dose calculations, revised. New York: The Societyof Nuclear Medicine.

Lomat L, Galburt G, Quastel MR, Polyakov S, Okeanov A, Rozin S. 1997. Incidence of childhood disease in Belarus associated with the Chernobyl accident. Environ Health Perspect. 105(Suppl 6): 1529–1532.

Lorber M. 2009. Use of a simple pharmacokinetic model to characterize exposure to perchlorate. J Expo Sci Environ Epidemiol. 19(3): 260–273.

Lötsch J. 2005. Pharmacokinetic-pharmacodynamic modeling of opioids. J Pain Symptom Manage. 29(5):90–103.

Macey R, Oster G, Zahnley T. 2009. Berkeley Madonna user's guide. Version 8.02. Berkeley (CA): University of California, Department of Molecular and Cellular Biology.

Marinelli L, Quimby E, Hine G. 1948. Dosage determination with radioactive isotopes: II. Practical considerations in therapy and protection. Am J Roentgenol Radium Ther Nucl Med. 59:260–280.

Matsunaga T, Kobayashi K. 2001. Sensitivity analysis on the deposition of inhaled radioactive iodine and the effectiveness of iodine prophylaxis. Jpn J Health Phys. 36(1):31–44.

Michalke B, Schramel P, Hasse S. 1996. Determination of free iodide in human serum: separation from other I-species and quantification in serum pools and individual samples. Mikrochim Acta. 122(1-2): 67–76.

National Cancer Institute 2015. Estimated exposure and thyroid doses report. [accessed 2021 May 15]. https://www.cancer.gov/about-cancer/causes-prevention/risk/radiation/i131-report-and-appendix.

[NCRP] National Council on Radiation Protection 2007. Development of a biokinetic model for radionuclide-contaminated wounds and procedures for their assessment, dosimetry and treatment. NCRP Report 156. Bethesda Maryland: National Council of Radiation Protection.

Rall JE, Robbins J, Lewallen CG. 1964. The thyroid. In: Pincus G, Thimann KV, Astwood EB, editors. The hormones. Physiology, chemistry, and applications. New York London: Academic Press; p. 159–440.

Ramsden D, Passant FH, Peabody CO, Speight RG. 1967. Radioiodine uptakes in the thyroid studies of the blocking and subsequent recovery of the gland following the administration of stable iodine. Health Phys. 13(6):633–646.

Reference.md 2020. Perchloracap. [accessed 2021 May 15]. http://www.reference.md/files/PE/PERCHLORACAP.html.

Reiners C, Drozd V, Yamashita S. 2020. Hypothyroidism after radiation exposure: brief narrative review. J Neural Transm (Vienna)). 127(11):1455–1466.

Reiners C, Schneider R. 2013. Potassium iodide (KI) to block the thyroid from exposure to I-131: current questions and answers to be discussed. Radiat Environ Biophys. 52(2):189–193.

Riggs DS. 1952. Quantitative aspects of iodine metabolism. Pharmacol Rev. 4(3):284–370.

Rump A, Eder S, Lamkowski A, Kinoshita M, Yamamoto T, Abend M, Shinomiya N, Port M. 2019. Development of new biokinetic-dosimetric models for the simulation of iodine blockade in the case of radioiodine exposure in man. Drug Res (Stuttg)). 69(11):583–597.

Rump A, Stricklin D, Lamkowski A, Eder S, Abend M, Port M. 2016. Reconsidering current decorporation strategies after incorporation of radionuclides. Health Phys. 111(2):201–208.

Rump A, Eder S, Hermann C, Lamkowski A, Kinoshita M, Yamamoto T, Abend M, Shinomiya N, Port M. 2021. A comparison of thyroidal protection by iodine and perchlorate against radioiodine exposure in Caucasians and Japanese. Arch Toxicol.. 95(7):2335–2350.

Schäuble S, Stavrum AK, Puntervoll P, Schuster S, Heiland I. 2013. Effect of substrate competition in kinetic models of metabolic networks. FEBS Lett. 587(17):2818–2824.

Sheiner LB, Stanski DR, Vozeh S, Miller RD, Ham J. 1979. Simultaneous modeling of pharmacokinetics and pharmacodynamics: application to d-tubocurarine. Clin Pharmacol Ther. 25(3): 358–371.

Simchowitz L. 1988. Interactions of bromide, iodide, and fluoride with the pathways of chloride transport and diffusion in human neutrophils. J Gen Physiol. 91(6):835–860.

Simon SL, Bouville A, Land CE, Beck HL. 2010. Radiation doses and cancer risks in the Marshall islands associated with exposure to radioactive fallout from Bikini and Enewetak nuclear weapons tests: Summary. Health Phys. 99(2):105–123.

Spetz J. 2010. Biodistribution of free 125 I, 131 I and 211 At in rats [Master of Science thesis]. Department of Radiation Physics, University of Gothenburg, Sweden.

[SSK] Strahlenschutzkommission 1998. Radiation protection principles for radioiodine therapy. Recommendation by the German Commission on Radiological Protection. Adopted at the 142nd session of the Commission on Radiological Protection on 5/6 December, 1996. In: Veröffentlichungen der Strahlenschutzkommission Band 40. Gustav Fischer Verlag.

[SSK] Strahlenschutzkommission 2018. Verwendung von Jodtabletten zur Jodblockade der Schilddrüse bei einem Notfall mit Freisetzung von radioaktivem Jod. Empfehlung der Strahlenschutzkommission. Verabschiedet in der 294. Sitzung der Strahlenschutzkommission am 26. April 2018. [accessed 2021 May 25]. https://www.ssk.de/SharedDocs/Beratungsergebnisse_PDF/2018/2018-04-26Jodmerk.pdf?__blob=publicationFile.

Suwansaksri N, Preechasuk L, Kunavisarut T. 2018. Nonthionamide drugs for the treatment of hyperthyroidism: From present to future. Int J Endocrinol. 2018:57940545794054. eCollection 2018. [accessed 2021 May 25]. https://www.researchgate.net/publication/324697060_Nonthionamide_Drugs_for_the_Treatment_of_Hyperthyroidism_From_Present_to_Future.

Verger P, Aurengo A, Geoffroy B, Le Guen B. 2001. Iodine kinetics and effectiveness of stable iodine prophylaxis after intake of radioactive iodine: a review. Thyroid. 11(4):353–360.

Wessels BW, Syh JH, Meredith RF. 2006. Overview of dosimetry for systemic targeted radionuclide therapy (StaRT). Int J Radiat Oncol Biol Phys. 66(2 Suppl):S39–S45.

Wolff J. 1964. Transport of iodide and other anions in the thyroid gland. Physiol Rev. 44:45–90.

Wolff J. 1998. Perchlorate and the thyroid gland. Pharmacol Rev. 50(1):89–105.

Wolff J. 1969. Iodide goiter and the pharmacologic effects of excess iodide. Am J Med. 47(1):101–124.

[WHO] World Health Organization 2017. Iodine thyroid blocking. Guidelines for use in planning for and responding to radiological and nuclear emergencies. Geneva: World Health Organization.

Yoshida S, Ojino M, Ozaki T, Hatanaka T, Nomura K, Ishii M, Koriyama K, Akashi M. 2014. Guidelines for iodine prophylaxis as a protective measure: information for physicians. Japan Med Assoc J. 57(3):113–123.